

Magnon-like Properties of 1D Spin-3/2 Chains

J. J. Hernández-Sarria^{a,b} and K. Rodríguez^a

^aDepartamento de Física, Universidad del Valle, A.A. 25360, Cali, Colombia;

^bCentre for Bioinformatics and Photonics—CIBioFi, Calle 13 No. 100-00, Edificio 320
No. 1069, Cali, Colombia

ABSTRACT

We study the magnon-like properties of the repulsively interacting spin-3/2 fermions in one-dimensional optical lattices at quarter filling. By means of the Holstein-Primakoff transformation performed on the spinor chain we obtain a spinless boson system described by an extended Bose-Hubbard model with a hole-like lowest band. The magnon model involves single, pair and correlated hopping between nearest neighbors beside the on-site and nearest neighbor interactions. The Mott-insulator phases of the spin-3/2 lattice fermions are mirrored with the magnon-like counterpart by analyzing several observables which should reveal these phases in state-of-the-art experiments. The numerical calculations are performed using the Exact Diagonalization and Matrix Product State formalism.

Keywords: Spinor gases, Bose-Hubbard, magnons, strongly-correlated systems

1. INTRODUCTION

At very low temperatures quantum spin systems are viewed as quantum simulators of interacting bosons since they share several macroscopic quantum behaviors such as superfluidity¹ and macroscopic quantum tunneling.² As it was pointed out, there is an exact correspondence between a quantum antiferromagnet and a lattice Bose gas³ and such analogy between spins and bosons has confirmed to be very advantageous bringing a link to the exceptional BEC phenomenon. Moreover, the bosonic description bring an innate understanding for complex quantum behaviors which are much less intuitive in the original spin terminology. This provides new viewpoints to critical problems and, hence, contribution to the understanding of new phenomena.

It has been shown that frustrated spin systems, where competing interactions cannot be simultaneously satisfied, offer the realization of exotic phases of strongly correlated bosons such as the spin liquid phase. This frustration can be classically treated when the spin S is larger than the minimum 1/2 and the system is driven by thermal energy choosing a random orientation from the different microstates and behaving as a liquid and when the temperature is small enough the spins are frozen out. But when the spin S is comparable to 1/2 the quantum mechanical uncertainty gives zero-point motions and the system presents quantum fluctuations arriving at the quantum spin liquid, hence the spins simultaneously points in many different directions involving wide entanglement between far apart particles.

In the past, spin-3/2 particles were considered as high-spin particles and therefore suitable for a classical treatment. But it has been proven their quantum-mechanical behavior and, in particular, in absence of an external magnetic field their interestingly hidden $SO(5)$ symmetry⁴ or in presence of a quadratic external field a hidden $SU(2) \otimes SU(2)$ symmetry.⁵ These high fermionic systems present exotic collective excitations absent in interacting electrons systems since there is an interplay between superfluidity and magnetism. This fact is due to the presence of different internal states⁶ reflected in the presence of spin-changing collisions precluded in spin-1/2 systems where there are solely spin-preserving collisions.

Ultracold gases in optical lattices constitute an extraordinary tool for the analysis of strongly-correlated gases under extremely well-controlled conditions.^{6,7} In this work, we study the magnon-like properties of repulsively

Further author information: (Send correspondence to K. R.)

J. J. H.-S.: E-mail: jhon.hernandez.sarria@correounivalle.edu.co

K. R.: E-mail: karem.c.rodriguez@correounivalle.edu.co

interacting spin-3/2 fermions in one-dimensional optical lattices.⁸ For large-enough interactions, the system enters into the Mott-insulator regime with maximally one fermion per site.

We perform a Holstein-Primakoff transformation to the fermionic system, expanding the spin operators in terms of the creation and annihilation operators of the harmonic oscillator, i.e. magnon-like position-operators. In this way, we obtain a spinless boson system described by an extended Bose-Hubbard model^{9–11} with a hole-like lowest band. The magnon-like model involves single, pair and correlated nearest neighbors hopping terms beside the on-site and nearest neighbor interactions. Lattice bosons and several transitions occurring in these systems have been studied extensively in ultracold atomic gases in optical lattices.

The magnetic phases present in the Mott-insulator of the spin-3/2 lattice fermions namely the gapless spin liquid and the gapped spin Peierls quantum phases, previously studied in Ref.^{4,5,12} are analyzed in the mirror frame of their bosonic counterpart.

This kind of work pave the path of revealing magnetic phases signatures in the state-of-the-art spinless boson experiments going beyond the physics of Bose-Einstein condensation and to look at the fascinating new quantum phases of interacting bosons on a lattice. The many-body numerical calculations are performed using the Matrix Product State formalism.¹³

2. MODELS UNDER CONSIDERATION

2.1 Generalized Heisenberg Hamiltonian (GHH)

We consider a balanced mixture of spin-3/2 fermions in a 1D lattice with $N_m = N_{-m}$, where N_m is the number of fermions with spin projection m , such that the magnetization vanishes, $\mathcal{M} \equiv \sum_m m N_m = 0$. With a harmonic trap along the lattice, the Mott-insulator phase occupy the central region. For a deep enough lattice and low filling, meaning single-band regime, the system Hamiltonian is modeled by the Hubbard model⁸ which describes 4-component fermions with equal masses interacting via contact potential. The interaction strengths $g_{0,2} = 4\pi\hbar^2 a_{0,2}/M$ characterize the s -wave channels with total spin $\{0, 2\}$ (the only available due to symmetry), with $a_{0,2}$ the scattering lengths and M the atomic mass. Although, typically a_0 and a_2 are similar, their values may be controlled by means of microwave dressing¹⁴ or optical Feshbach resonances.¹⁵ Along this paper, we use the following change of variables:⁵ $G = (g_0 + g_2)/2 = 1$ (being the unity) and $g = (g_2 - g_0)/(g_2 + g_0)$, where g gives a measurement of the spin-changing collision strength. The interactions preserve \mathcal{M} and the linear Zeeman effect induced by a magnetic field does not play any role.

For large-enough interactions, $G \gg t$, we may consider the hard-core case, with maximally one fermion per site. For a chemical potential μ larger than a critical $\mu_c(t)$ the system enters into the Mott-insulator regime with one fermion per site. We focus below in the properties of these magnetic phases. Within the Mott regime we perform perturbation theory in the hopping term (t) obtaining a low-energy effective hyperfine spin model Hamiltonian in the strong-coupling limit. The virtual tunneling of particles induces effective spin-exchange interactions between nearest neighbor sites, as a result a generalized Hubbard Hamiltonian⁸ is obtained,

$$\hat{H}_{\text{GHH}} = \sum_i \left[\alpha_1 (\vec{S}_i \cdot \vec{S}_{i+1}) + \alpha_2 (\vec{S}_i \cdot \vec{S}_{i+1})^2 + \alpha_3 (\vec{S}_i \cdot \vec{S}_{i+1})^3 + \alpha_4 I_i \right], \quad (1)$$

the physics of the Hubbard model passes through to the Heisenberg model by the coefficients $\alpha_{1,2,3,4}$ given by,¹⁶

$$\begin{aligned} \alpha_1 &= -\frac{t^2}{24} \left(\frac{31}{1-g} + \frac{23}{1+g} \right), & \alpha_2 &= \frac{t^2}{18} \left(\frac{5}{1-g} + \frac{17}{1+g} \right), \\ \alpha_3 &= \frac{2}{9} t^2 \left(\frac{1}{1-g} + \frac{1}{1+g} \right), & \alpha_4 &= -\frac{33}{32} t^2 \left(\frac{1}{1-g} + \frac{5}{1+g} \right). \end{aligned} \quad (2)$$

When the charge gap opens, the insulating ground-state phases are located in the repulsive interaction regime $g_{F=0,2} > 0$ where the Hamiltonian presents two distinct magnetic phases. In terms of the previously introduced variable g and in absence of an external field,^{12,17} the ground-state of the system for $-1 < g \leq 0$ is a gapless spin-liquid (SL) phase with three gapless spin-modes, including the exactly solvable $SU(4)$ point ($g = 0$).¹⁸ For $0 < g < 1$ the ground-state is a spin-Peierls (SP) phase, which exhibits a spin gap and long-range dimerization order. At $g = 0$, the system undergoes a Kosterlitz-Thouless-like transition between the two phases.¹⁹

2.2 Extended Bose-Hubbard Hamiltonian (EBHH)

Holstein and Primakoff²⁰ introduced a very useful technique which formalizes the harmonic-oscillator behavior of a spin system. Their approach is based on the expansion of the spin operators in terms of the bosonic creation and annihilation operators,

$$\vec{S}_i^- = \sqrt{2S} \hat{b}_i^\dagger, \quad \vec{S}_i^+ = \sqrt{2S} \hat{b}_i, \quad \hat{n}_i = S - \hat{S}_{z,i}, \quad (3)$$

where $S = 3/2$.

Using the previous set of transformations on the generalized Heisenberg Hamiltonian, Eq.(1), we obtain an effective model for the case of a finite (though vanishingly small) bosonic density, performing a truncation upto four operators following the $1/S$ leading order. This dilute gas of bosons brings us a magnon-like Hamiltonian in position space of the form,

$$\hat{H}_{EBHH} = \sum_i \left\{ -t_1 \left(\hat{b}_i^\dagger \hat{b}_{i+1} + \text{h.c.} \right) + U_0 \hat{n}_i (\hat{n}_i - 1) - \mu \hat{n}_i + U_1 \hat{n}_i \hat{n}_{i+1} \right. \\ \left. - t_2 \left(\hat{b}_i^{\dagger 2} \hat{b}_{i+1}^2 + \text{h.c.} \right) + U_2 \left(\hat{b}_i^\dagger \hat{n}_i \hat{b}_{i+1} + \hat{b}_i^\dagger \hat{n}_{i+1} \hat{b}_{i+1} + \text{h.c.} \right) \right\}, \quad (4)$$

this extended Bose-Hubbard Hamiltonian involves several terms such as single (t_1), pair (t_2) and correlated (U_2) hopping between nearest neighbors, beside the on-site (U_0) and nearest-neighbor (U_1) interactions. The coefficients are given by the following expressions,

$$t_1 = -2 \left(\frac{t^2}{1+g} \right), \quad U_0 = \frac{3}{2} \left(\frac{t^2}{1+g} \right), \quad \mu = 2 \left(\frac{t^2}{1+g} \right), \quad U_1 = \frac{2}{3} t^2 \left(\frac{1}{1-g} + \frac{10}{1+g} \right), \\ t_2 = -\frac{3}{2} \left(\frac{t^2}{1+g} \right), \quad U_2 = t^2 \left(\frac{1}{1-g} - \frac{1}{1+g} \right). \quad (5)$$

The positive hopping term, t_1 , shows that we have a hole-like band, suggesting that the minima are located at $\pm\pi/a$, in contrast to the particle-like band where the minimum is located at 0, where a is the lattice constant.

Since the transformation is not linear and the coupling between the oscillators has important consequences for many properties of ordered systems, we calculate the ground and low lying energy states as a function of the spin-changing collision strength, g , in this magnon-like frame-work.

It is worth mentioning that due to the two-sites ($i, i+1$) character of the Hamiltonian (1), it is necessary to have a special care for the single-site terms retrieved by the transformation, making them doubled in the bulk and singled in the borders. This is actually the reason why the U_0 of the bosonic Hamiltonian (4) here presented does not have the usual one half coefficient to avoid further complications.

2.3 Truncated spin Hamiltonian (TSH)

To retrieve the extended Bose-Hubbard model, we have implemented a consideration in the mathematical procedure that allow us to simplify the problem, namely keeping only upto four operators. This approximation restricts the information of the original system and induces some errors. In order to estimate the information lost to analyze the validity of our results, we have perform a Holstein-Primakoff back-transformation to go from the extended Bose-Hubbard model to a spin system. Hereafter, we address this model as the truncated spin Hamiltonian which is given by the following expression,

$$\hat{H}_{TSH} = \sum_i \left\{ J \left(\vec{S}_i^+ \cdot \vec{S}_{i+1}^- + \vec{S}_i^- \cdot \vec{S}_{i+1}^+ \right) + U_1 \hat{S}_i^z \cdot \hat{S}_{i+1}^z - \frac{t_2}{9} \left[\left(\vec{S}_i^+ \right)^2 \cdot \left(\vec{S}_{i+1}^- \right)^2 + \left(\vec{S}_i^- \right)^2 \cdot \left(\vec{S}_{i+1}^+ \right)^2 \right] \right. \\ \left. - \frac{U_2}{3} \left(\vec{S}_i^+ \cdot \vec{S}_{i+1}^- + \vec{S}_i^- \cdot \vec{S}_{i+1}^+ \right) \cdot \left(\hat{S}_i^z + \hat{S}_{i+1}^z \right) + B \hat{S}_i^z + U_0 \left(\hat{S}_i^z \right)^2 + C \hat{I}_i \right\}, \quad (6)$$

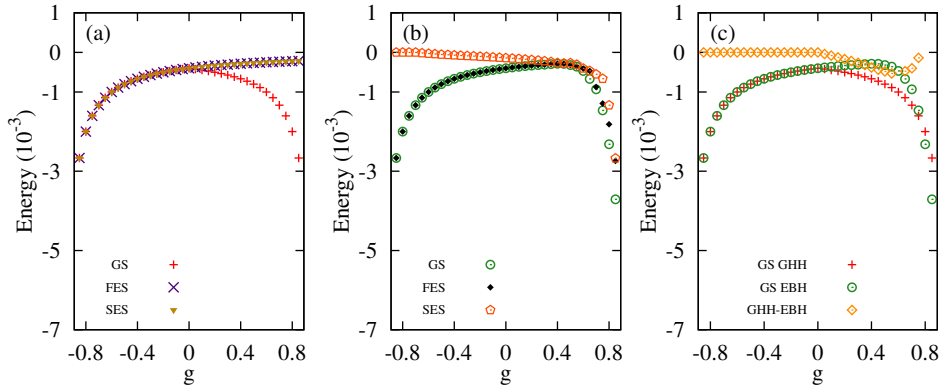


Figure 1. Energy of the ground-state (GS), first (1st) and second (2nd) excited states as a function of the spin-changing collision strength, g , for (a) the spin model (GHH) and (b) the bosonic model (EBHH). (c) Direct comparison between the ground-state of the GHH and EBHH, the relative error of the Holstein-Pimakoff transformation is shown with orange diamonds.

where the coefficients t_2, U_0, U_1 and U_2 are the same of Eq. (5), and the remaining coefficients are given by,

$$J = \frac{2}{3}t_2 \left(\frac{2}{1-g} - \frac{1}{1+g} \right), \quad B = -2t_2 \left(\frac{1}{1-g} + \frac{14}{1+g} \right), \quad C = 3t_2 \left(\frac{1}{1-g} + \frac{9}{1+g} \right). \quad (7)$$

3. TWO-SITES PROBLEM

3.1 GHH vs EBHH

We now solve the interacting EBHH, Eq. (4), for the two-sites problem in position space by means of Exact Diagonalization and compare the energy results with the spectrum of the already diagonalized spin system.¹⁶ We solve the two-sites problem despite the fact that the small system size introduces several symmetries that the thermodynamic-limit does not involve. Nevertheless, we consider this as a way to gain experience with the models and develop new strategies to approach them for longer system sizes. The retrieved data solving the bosonic system is observed in figure 3.1, where the ground-state, first and second excited states are plotted as a function of the spin-changing collision parameter, g , in panel (a) for the spin system of section 2.1 and in panel (b) for the bosonic system of section 2.2. Panel (c) shows explicitly the comparison among the ground-states of the two models. This third panel is very interesting because of the marvelous agreement of both descriptions in the spin-liquid regime ($g \leq 0$). Before commenting about the disagreement in the dimerized region, it is important to point out that the energy scale used to present the results is of the order of 10^{-3} . In this spin-Peierls phase ($g > 0$) the deviations of the bosonic model from the spin one are notorious, one can observe that the existing symmetry around $g = 0$ has been broken although the functional form is still conserved with the maximum energy value shifted to the right around $g \sim 0.6$. The discrepancy in the energy is clearly originated by the truncation of the Hamiltonian and the explanation arises in the fact that this magnetic phase presents a long-range-order which means is highly correlated, therefore any missing information (even of small order) may lead to a detour of the intrinsic properties. Based on the difference between the ground-state energies of each model, we can quantize the relative error carry out by the transformation in each phase: for the spin-liquid phase there is no error whatsoever and for the spin-Peierls as can be appreciated in figure 3.1(c) is of the order of 10^{-3} for $g = 0.6$ and 10^{-6} for $g = 0.2$.

3.2 GHH - EBHH and TSH

In the following, the energy spectrum of the truncated spin system is compared with the original generalized Heisenberg spectrum of the spin-3/2 particles (GHH) and the extended Bose-Hubbard system (EBHH), the analysis is summarized in figure 3.2. It is interesting to point out, that some of the thermodynamic-limit features of the magnetic phases are recovered in this truncated model solved for two-sites. Such features are the double degeneracy of the spin-Peierls ground-state and the singlet ground-state in the spin-liquid phase.

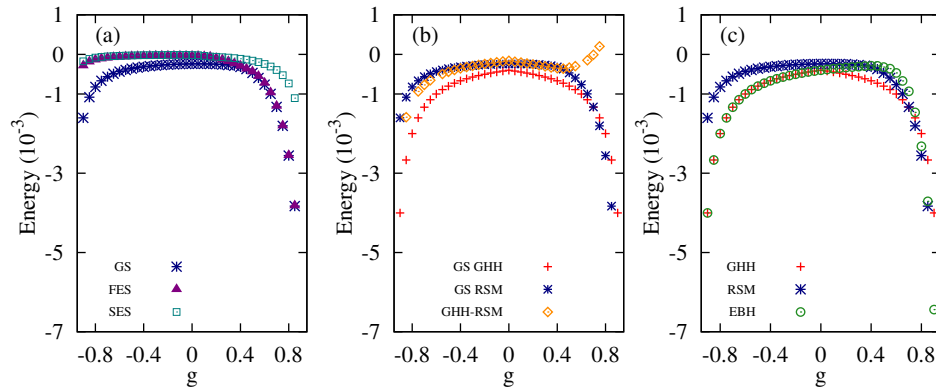


Figure 2. Comparison between the two spin models: the original GHH and the truncated back-from-bosons spin system TSH. (a) GS and low-lying energy levels for the TSH. (b) Ground-state energy comparison between GHH and TSH, the relative error of the two consecutive transformations is shown with orange diamonds. (c) The full comparison among the three models analyzed by the two-sites problem, spin systems: GHH and TSH and bosonic system: EBHH.

Commonly, this is lost as it was shown in section 3.1 due to the large amount of extra-symmetries that small systems introduce to the eigen-problem.

In the figure 3.2(a) we observed that the ground-state energy together with the “first excited” state are degenerated in the dimerized region, where $g > 0$. Furthermore, the energy gap, which is the separation between these degenerated ground states with the next state, grows as the interaction parameter g increases. In the spin-liquid phase, where $g < 0$, it is observed a single ground state and the energy gap grows as g grows in absolute value. This indicates that the energy gap in both magnetic phases depends strongly on the interaction strength in both spin-channels. In the dimerized spin-Peierls phase, the energy gap grows as the interaction strength of channel $F = 2$ (g_2) is bigger than the channel $F = 0$ (g_0). Whereas in the spin-liquid phase the opposite occurs, and the gap opens when the g_0 strength is stronger.

In panel (b), it is shown the ground states for the two studied spin systems: the Heisenberg (red crosses) and the truncated (blue asterisks) models, additionally, the difference among them is also presented by orange diamonds. The discrepancy is minimal where the super-exchange interaction vanishes, $g = 0$, showing that the loss of information provided by the Holstein-Primakoff transformation does not play a major role at the lack of g and all models mirror each other. Elsewhere the strong dependency with the interactions makes the models unfaithful up to three orders of magnitude, although keeping the data functional form.

In panel (c), we present the ground-state energy for the three systems under consideration, GHH, EBHH and TSH. We had seen that the transformation to bosonic operators maintains the ground-state energy value in the spin-liquid regime. Nevertheless, a further inverse transformation to spins shows a rising energy and therefore some information is lost in this phase. On the other hand, in the dimerized spin-Peierls phase both models EBHH and TSH present ground-state energy values very close to each other and, what is more, the values tend to be close to the GHH values for $g \leq 0.5$, suggesting that for larger values of g (still smaller than one), the models resemble each other again.

3.3 Validity of the transformation

Then, we can conclude that the validity of the transformations is higher: first, when there is a lack of super-exchange interaction, $g = 0$ and the system is in the spin-liquid phase, and second, when g is positive and large but still smaller than one, $0.6 < g \lesssim 1$. Therefore, the validity strongly depends on the super-exchange interaction g and the best results are found for the spin-liquid phase, which is not a surprise since this is a “disorganized” phase shown in its liquid character in comparison with the dimerized phase that exhibits a long-range dimer order.

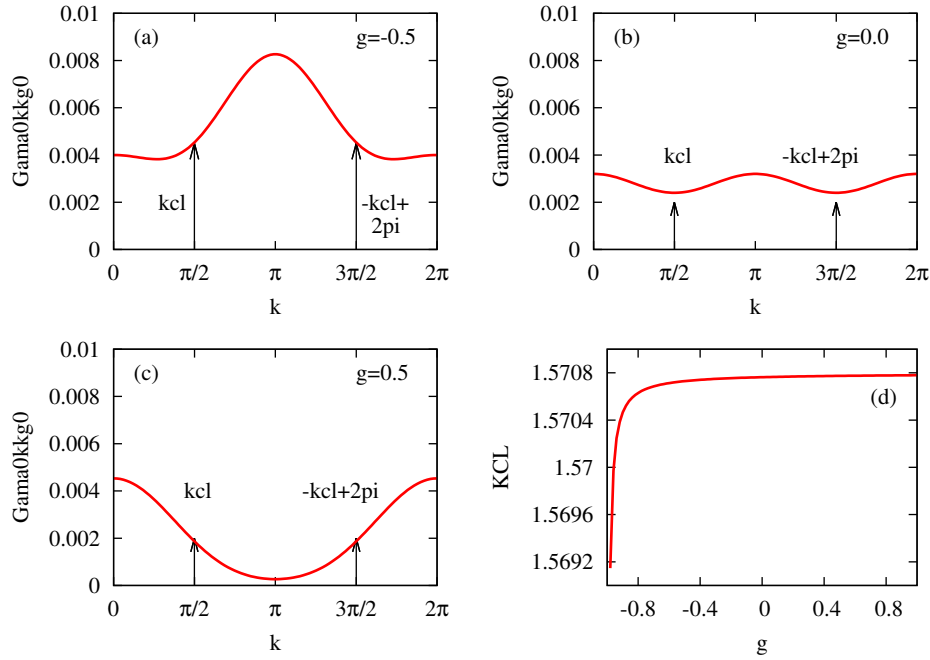


Figure 3. Vertex function $\Gamma(0; k, k)$ for several values of g in the two magnetic phases: on one hand, the spin-liquid phase when $g \leq 0$ ((a) $g = -0.5$ and (b) $g = 0$). On the other hand, the dimerized spin-Peierls phase when $g > 0$ ((c) $g = 0.5$). Panel (c) shows the slight change of k_{cl} as function of g .

4. MAGNON HAMILTONIAN

In order to analyze the actual magnons involved in the original spin system (GHH) of Eq. (1), a Fourier transform is performed on the generalized Bose-Hubbard Hamiltonian, \hat{H}_{EBHH} of Eq. (4), where the transformation on the bosonic operators is defined by

$$\hat{b}_j = \frac{1}{\sqrt{N}} \sum_k \hat{b}_k \exp(i\vec{k} \cdot \vec{r}_j), \quad (8)$$

and the creation operator is defined likewise. Here, the wave vector \vec{k} is defined in the Brillouin zone for the lattice and \vec{r}_j correspond to the particle position at site j . Substituting the ladder operators into the Hamiltonian and neglecting higher terms in bosonic operators according to the spirit of the $1/S$ expansion, we obtain a quadratic Hamiltonian given by

$$\hat{H}_M = \sum_k (2S\epsilon_k - \mu) \hat{a}_k^\dagger \hat{a}_k + \sum_{k, k', q} \frac{\Gamma_0(q; k, k')}{2L} \hat{a}_{k+q}^\dagger \hat{a}_{k'-q}^\dagger \hat{a}_k \hat{a}_{k'},$$

where the single magnon dispersion is

$$\epsilon_k = -\frac{t_1 \cos(k)}{S} = \frac{2t^2 \cos(k)}{g_2 S}. \quad (9)$$

And the bare interaction vertex is given by $\Gamma_0(q; k, k')$

$$\Gamma_0(q; k, k') = 4t_2 \cos(k + k') + U_0 + 2U_1 e^{iq} + 4U_2 [\cos(k') + \cos(k + q)]. \quad (10)$$

When there is zero transferred momenta, $q = 0$, and the incoming and outgoing momenta are equal, $k = k'$, the interaction vertex modifies as

$$\Gamma(0; k, k) = 4t_2 \cos(2k) + 8U_2 \cos(k) + 2U_1 + U_0. \quad (11)$$

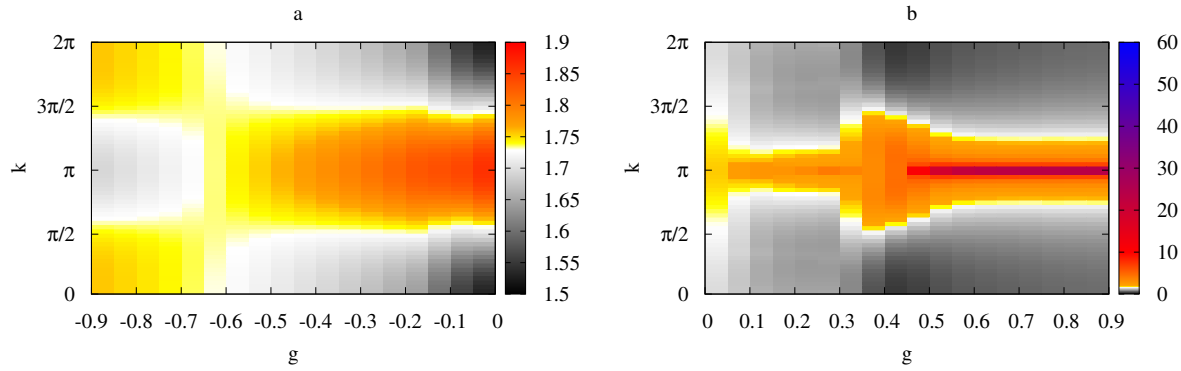


Figure 4. Momentum distribution as a function of the super-exchange interaction strength g , (a) in the spin-liquid phase, $g < 0$, and (b) in the dimerized spin-Peierls phase, $g > 0$.

Furthermore, in absence of spin-changing collisions, $g = 0$, the minima are obtained at $k_{cl} = \pm \arccos(-J'/4)$ as it is expected following.²¹ In the present system $J' = -t_1/S$, see figure 3. The bosons tend to condensate at the minimum of the single-particle dispersion since they experience a minimal repulsion there. In figure 3, one can appreciate how the position of this minimum changes as a function of g . It is shown in panel (a) that the minimum position is located where $k_{cl} < \pi/2$, in panel (b) we see that in absence of spin-changing collisions, $g = 0$, the minima are at $k_{cl} = \pi/2 \pm 2\pi$ and panel (c) shows one minimum at $k_{cl} = \pi$. It is relevant the case of $g \leq 0$ where permanently there are two minima.

To look in more detail this magnon dispersion-relation behavior in the system, we have performed numerical calculations using the Matrix Product States (MPS) formalism¹³ with 60 sites, open boundary conditions, and matrix dimension 20. The momentum distribution for the magnon system in the two distinct phases as a function of g are presented in figure 4. In panel 4(a) we can appreciate that in the window $-1 \lesssim g < -0.6$ the system presents two minima in the dispersion as was suggested in the classical case (figures 3(a) and 3(b)) but these minima move to each other and meet at $k = \pi$ around $g \sim -0.5$ and henceforth there is solely one minimum until the end of the dimerized phase $g \lesssim 1$.

5. SUMMARY

In conclusion, the position-space magnons obtained, by means of the Holstein-Primakoff transformation from a repulsively interacting spin-3/2 fermions, shows a high-quality energy spectrum, for the ground and low-lying states, in comparison with the original spin system for the two-sites problem. The magnon-like spectrum resembles the functional form and the energy-scale showing the reproducibility in actual spinless-bosons experiments. We show that the validity of the transformation increases in absence of spin-changing collisions processes, this point corresponds to the spin-liquid phase. On the other hand the transformation has also a high validity then the super-exchange interaction is positive and close to its maximal value, corresponding to the dimerized spin-Peierls phase. The accuracy of the transformation is strongly linked to the fermionic hopping parameter t and the deeper the spin-3/2 systems is in the Mott-insulator regime, the truthful the transformation is.

We have also studied the magnon dispersion-relation behavior in the classical limit as M. Arlego et. al.²¹ and the exact case by means of the MPS formalism and conclude that in the spin-liquid phase the dispersion-relation presents two minima emphasizing the liquid nature of this phase, and one minimum exclusively in the spin-Peierls phase. The two minima at the gapless phase do not persist all the way up to $g = 0$ as the classical picture suggests but they cease around $g \sim -0.5$ where they merge and stick together up to the far end ($g \lesssim 1$) of the dimerized phase.

ACKNOWLEDGMENTS

The authors acknowledge Universidad del Valle for funding under grant CI 7973 and the Excellence Center of New Materials (CENM) for financial support of the research group. J. J. H.-S. acknowledges support from CIBioFi, and the Colombian Science, Technology and Innovation Fund-General Royalties System (Fondo CTeI-SGR) under contract No. BPIN 2013000100007.

REFERENCES

- [1] T. Giamarchi, C. Rüegg, and O. Tchernyshyev *Nature Physics* **4**, p. 198, (2008).
- [2] E. M. Chudnovsky and L. Gunther *Phys. Rev. Lett* **60**, p. 661, (1988).
- [3] T. Matsubara and H. Matsuda *Prog. Theor. Phys* **16**, pp. 569–582, (1956).
- [4] C. Wu, J. P. Hu, and S. C. Zhang *Phys. Rev. Lett* **91**, p. 186402, (2003).
- [5] K. Rodríguez, A. Argüelles, M. Colomé-Tatché, T. Vekua, and L. Santos *Phys. Rev. Lett* **105**, p. 050402, (2010).
- [6] I. Bloch, J. Dalibard, and W. Zwerger *Rev. Mod. Phys* **80**, p. 885, (2008).
- [7] M. Lewenstein, A. Sanpera, and V. A. B. Damski *et al.*, *Adv. Phys* **56**, pp. 243–379, (2007).
- [8] H.-H. Tu, G.-M. Zhang, and L. Yu *Phys. Rev. B* **74**, p. 174404, (2006).
- [9] F. M. E. Plekhanov and G. Sica *Eur. Phys. J. B* **86**, p. 408, (2013).
- [10] W. Zhang, R. Yin, and Y. Wang *Phys. Rev. B* **88**, p. 174515, (2013).
- [11] K. Kapcia, S. Robaszkiewicz, and R. Micnas *J. Phys* **24**, p. 215601, (2012).
- [12] C. Wu *Phys. Rev. Lett* **95**, p. 266404, (2005).
- [13] F. Verstraete, J. Garcia-Ripoll, and J. I. Cirac *Phys. Rev. Lett* **93**, p. 207204, (2004).
- [14] D. J. Papoular, G. V. Shlyapnikov, and J. Dalibard *Phys. Rev. A* **81**, p. 041603, (2009).
- [15] P. O. Fedichev, Y. Kagan, G. V. Shlyapnikov, and J. T. M. Walraven *Phys. Rev. Lett* **77**, p. 2913, (1996).
- [16] (doi:10.1007/s10948-015-3104-8).
- [17] P. Lecheminant, E. Boulat, and P. Azaria *Phys. Rev. Lett* **95**, p. 240402, (2005).
- [18] B. Sutherland *Phys. Rev. B* **12**, p. 3795, (1975).
- [19] C. Wu *Mod. Phys. Lett. B* **20**, pp. 1707–1738, (2006).
- [20] T. Holstein and H. Primakoff *Phys. Rev* **58**, p. 1098, (1940).
- [21] M. Arlego, F. Heidrich-Meisner, A. Honecker, G. Rossini, and T. Vekua *Phys. Rev. Lett* **84**, p. 224409, (2011).